Published by SET Publisher

Journal of Basic & Applied Sciences

ISSN (online): 1927-5129

Geodynamics of the Caucasus – Anatolian-Arabian region and Turkey-Syria Earthquakes 2023

Svalova Valentina*

Sergeev Institute of Environmental Geoscience, Russian Academy of Sciences, 13, building 2 Ulansky per., Moscow 101000, Geophysical Institute, Vladikavkaz Scientific Center, Russian Academy of Sciences, 93a Markova Str., Vladikavkaz 362002, Russian Federation

Article Info:

Keywords:
Earthquake,
geodynamics,
lithosphere,
Caucasus,
Turkey,
modeling.

Timeline:
Received: March 26, 2023
Accepted: April 20, 2023
Published: May 02, 2023

Citation: Valentina S. Geodynamics of the caucasus – anatolian-arabian region and turkey-syria earthquakes 2023. J Basic Appl Sci 2023; 19: 40-59.

Abstract:
The activation of natural disasters in the world requires the development of new approaches to the study of geological processes, in particular, at the boundaries of lithospheric plates, characterized by earthquakes, increased seismicity, volcanism, landslide processes, tsunamis and other dangerous natural processes and hazards. Earthquake of M 7.8 struck south - eastern Turkey and north - western Syria on 6 February 2023. The M 7.8 earthquake is the largest in Turkey since the 1939 Erzincan earthquake, and the second-strongest recorded in the country, after the 1668 North Anatolia earthquake. More than 52,800 deaths were confirmed: more than 46,100 in Turkey, and more than 6,700 in Syria. It is the deadliest natural disaster in Turkey's modern history. The earthquakes caused over US$100 billion in damages. The geodynamic models construction for the deep structure of natural hazards regions is an important contribution to the study of active continental margins, which is necessary for the earthquake forecast, prediction and prognosis, assessing geoecological risks and preparing population actions in the event of natural disasters and catastrophes. The Caucasus - Arabian region is a complex highly-stressed geodynamic structure, characterized by increased heat flow, high seismicity, magmatism and volcanism. The geodynamics of the Caucasus - Arabian region is determined by the collision of the Eurasian and Arabian lithosphere plates, as well as the complex history of the development of the Alpine-Himalayan belt and surrounding territories. The problem solution of geological structures formation and evolution in various complex geodynamic settings and natural hazards forecast and prognosis requires an analysis of all available geological - geophysical data, as well as the formulation and solution of problems of mechanical and mathematical modeling. Slow lithospheric deformations are simulated by models of viscous flow in multi-layered, incompressible, high-viscosity Newtonian fluid, using Navier-Stocks equation and discontinuity equation. The solution of the inverse problem of geodynamics by the direct method is developed. The first inverse problem of geodynamics was solved - the restoration of the velocity fields, pressures and stresses at the depth of the lithosphere according to the available data on the velocities on the surface. The second inverse problem of geodynamics has been posed and solved - the determination of the movement of boundaries at the depth of the lithosphere based on the given movements of the surface. The solutions obtained can be used to analyze deep geodynamic problems, and together with geothermal modeling, geological and geophysical methods and seismic tomography can serve as a reliable apparatus for studying deep geodynamics due to the formation and evolution of geological structures and the lithosphere stress-strain state researches. The solution of the problem is analyzed on the example of the Caucasus - Arabian region geodynamics. The Geodynamic concept of geoenvironment has been developed. Geodynamic models of the regions of hazardous natural processes in order to predict and prevent natural disasters and catastrophes are constructed. An algorithm for creating monitoring systems is suggested.

DOI: https://doi.org/10.29169/1927-5129.2023.19.04

*Corresponding Author
E-mail: v-svalova@mail.ru

1. INTRODUCTION

After every huge natural catastrophe the question of prognosis, forecast, reasons and monitoring arises. New systems of monitoring and scientific and emergency organizations will be suggested in the countries. New approaches to the problem of the earthquakes prognosis and prediction must be elaborated. The results of event must be analyzed at the new scientific level on the base of new geological-geophysical data. Huge victims demand new efforts for the problems decision – long-term, medium-term and short- term forecasts of disasters and earthquake resistant construction.

One of important steps could be elaboration of geodynamic model of the region of catastrophic event as basis for all possible geological-geophysical data collection and analysis at different scale with aim of future forecast, prediction and prognosis.

2. 2023 TURKEY–SYRIA EARTHQUAKE.

Earthquake of M 7.8 struck south -eastern Turkey and north - western Syria on 6 February 2023, at 04:17 of local time. The epicenter was 37 km west–northwest of Gaziantep. The earthquake hypocenter was at a depth of 10.0 km according to USGS. The earthquake was followed by a M 7.7 earthquake at 13:24. This earthquake was centered 95 km north-northeast from the first.

The M 7.8 earthquake is the largest in Turkey since the 1939 Erzincan earthquake of the same magnitude, and the second-strongest recorded in the country, after the 1668 North Anatolia earthquake. It is also one of the strongest earthquakes ever recorded in the Levant. There were more than 10,000 aftershocks in the three weeks that followed. The seismic sequence was the result of shallow strike-slip faulting.

There was widespread damage in an area of about 350,000 km. An estimated 14 million people (16 percent of Turkey's population) were affected. About 1.5 million people were left homeless.

More than 52,800 deaths were confirmed: more than 46,100 in Turkey, and more than 6,700 in Syria. It is the deadliest earthquake in Turkey since the 526 Antioch earthquake; deadliest in Syria since the 1822 Aleppo earthquake; deadliest worldwide since the 2010 Haiti earthquake; and the fifth-deadliest of the 21st century. It is the deadliest natural disaster in Turkey's modern history. The earthquakes caused over US$100 billion in damages (the fourth-costliest earthquakes).

The location of the earthquake is connected with a triple junction between the Anatolian, Arabian, and African plates (Figures **1-4**).

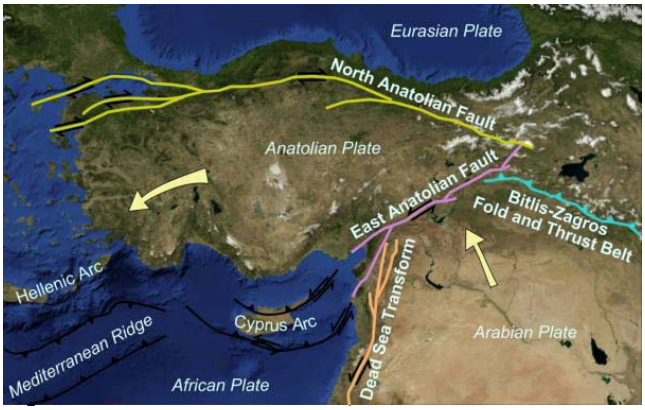

Figure 1: The largest systems of active faults in the Middle East: North Anatolian - Zagros and Levant - East Anatolian.

https://ru.wikipedia.org/wiki/Восточно-Анатолийский_разлом#/media/Файл:Anatolian_Plate.png

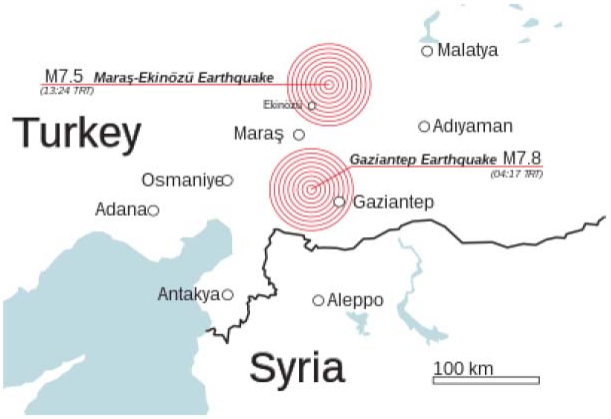

Figure 2: Epicenter locations of the first and second major earthquakes.

https://en.wikipedia.org/wiki/File: 2023_Gaziantep-Marash_Earthquakes.svg

The East Anatolian Fault traces the westward movement of Turkey to the Aegean Sea. The Dead Sea Transform traces the northward motion of the Arabian Peninsula, relative to the Africa and Eurasia plates.

The East Anatolian Fault is a 700-kilometre-long northeast–southwest left-lateral transform fault and forms the boundary between the Anatolian and Arabian plates. This intracontinental transform fault is the second largest strike-slip fault in Turkey.

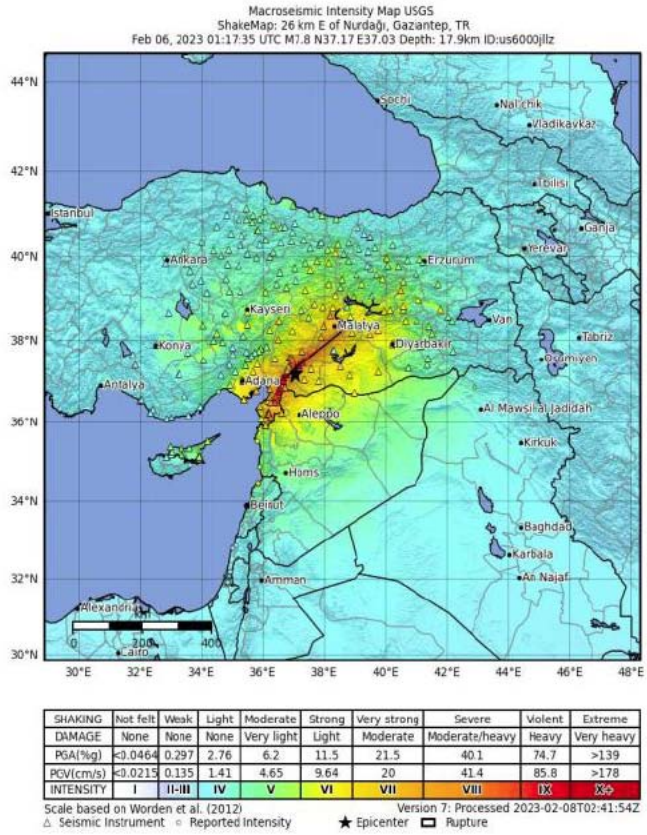

Figure 3: Distribution of the intensity of an earthquake of magnitude 7.8 with an epicenter near the city of Gaziantep. M_w 7.8 earthquake at 01:17 UTC (USGS).

The fault slip rates decrease from the east at 10 mm per year to the west of 1–4 mm per year. The fault produced large earthquakes in 1789 (M 7.2), 1795 (M 7.0), 1872 (M 7.2), 1874 (M 7.1), 1875 (M 6.7), 1893 (M 7.1), and 2020 (M 6.8).

The region of the 6 February 2023 earthquakes is relatively quiet seismologically (Figure **5**).

Geodynamic activity of the East Anatolian Fault is well investigated [12] (Figures **6-8**).

Only five earthquakes (1905, 1945, 1986, 1998) of magnitude 6.0 or larger have occurred there since 1905.

All these earthquakes occurred along or in the vicinity of the East Anatolian Fault. At the same time southern Turkey and northern Syria had significant and damaging earthquakes in the past. Aleppo, the second-largest city in Syria, was devastated several times historically by large earthquakes. Aleppo was struck by an estimated magnitude 7.1 earthquake in 1138 and an estimated magnitude 7.0 earthquake in 1822. Fatality estimates of the 1822 earthquake were 20,000–60,000.

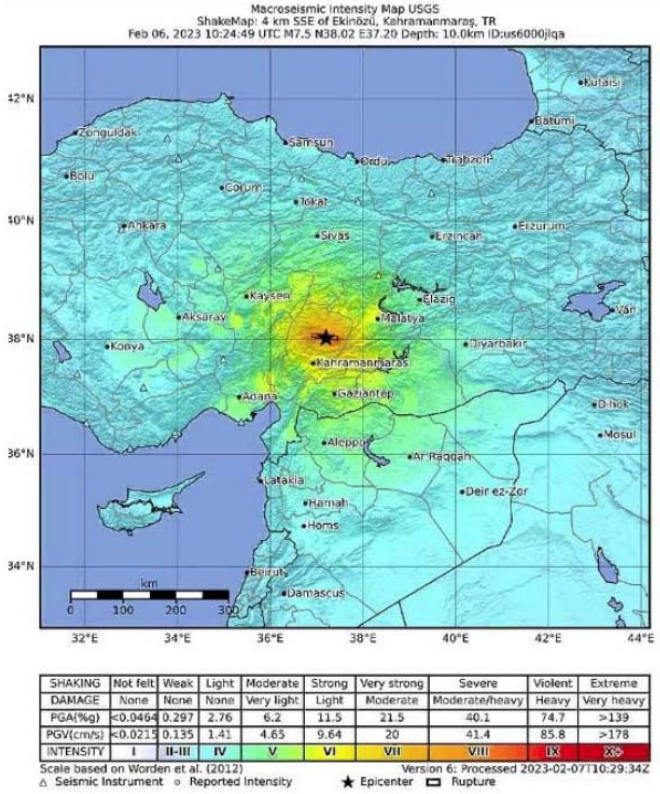

Figure 4: Strong ground motion map. Kahramanmarash earthquake. M_w 7.7 earthquake at 10:24 UTC (USGS).

In 1114, the city of Marash suffered an earthquake which killed 40,000. Major earthquakes affecting the Middle East in 856, 1033 and 1754 have resulted in 200,000, 70,000 and 40,000 deaths, respectively.

3. STUDY OF SEISMIC ACTIVITY OF THE NORTH ANATOLIAN FAULT ZONE

On August 17, 1999, the devastating Izmit earthquake struck Turkey. Its magnitude was 7.7, the epicenter was at a depth of 17 km near the city of Izmit, 80 km east of Istanbul. According to official figures, the death toll was about 15,000 people, about 25,000 were injured, and 600,000 lost their homes. Damage from the earthquake was initially estimated at more than 25 billion dollars, but later increased by another 5-7 billion. The shocks were also felt in neighboring countries.

The North Anatolian Fault, the first largest strike-slip fault in Turkey, produced 11 large earthquakes during the 20th century (Figure **9**).

Turkey is located in a seismically hazardous zone, its territory is crossed by the active North Anatolian Fault Zone (NAFZ), which separates the Eurasian and Anatolian tectonic plates, sliding relative to each other at a speed of 2 cm per year. Earthquakes constantly

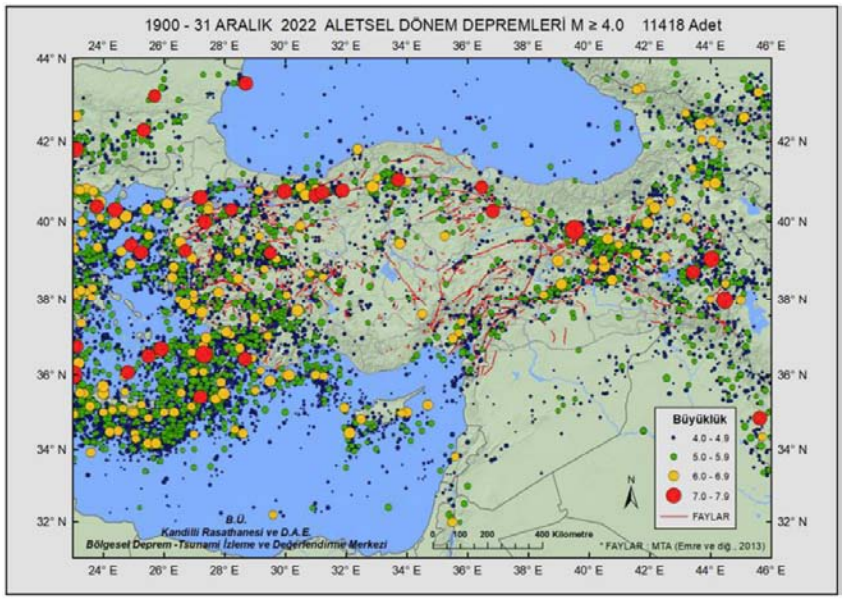

Figure 5: Seismicity map of Turkey and nearby regions for the period from 1900 to 2022.
(Regional Earthquake-Tsunami Monitoring Center, Boğaziçi University).

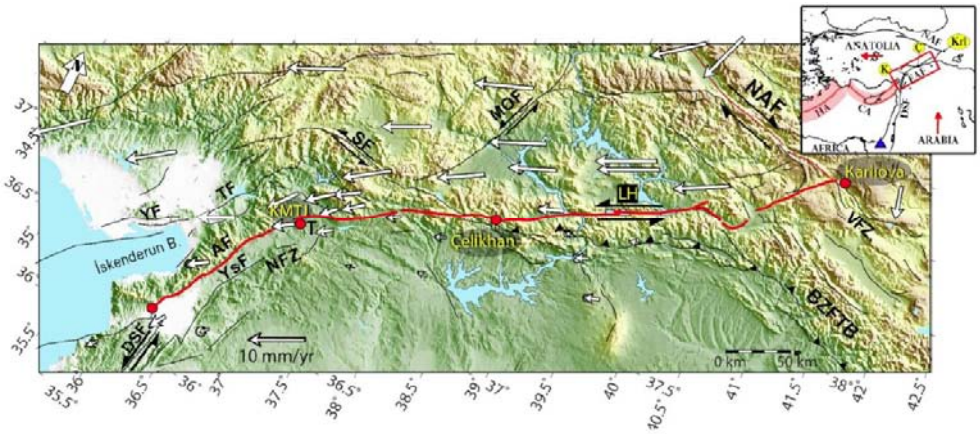

Figure 6: Tectonic setting in the region of the East Anatolian Fault (indicated by a bright red line). The black arrows along the axis indicate the relative motion of the fault walls. The white arrows indicate the speeds of movement in a fixed frame of reference, determined using GPS (the length of the arrows indicates the magnitude of the speed) [12].

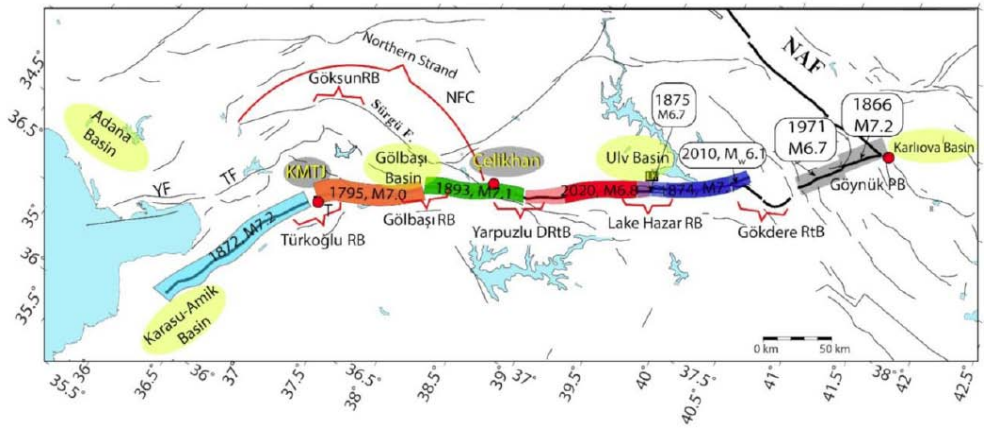

Figure 7: Sites on the East Anatolian Fault, showing the dates and epicenters of the largest earthquakes before the event of February 6, 2023 [12].

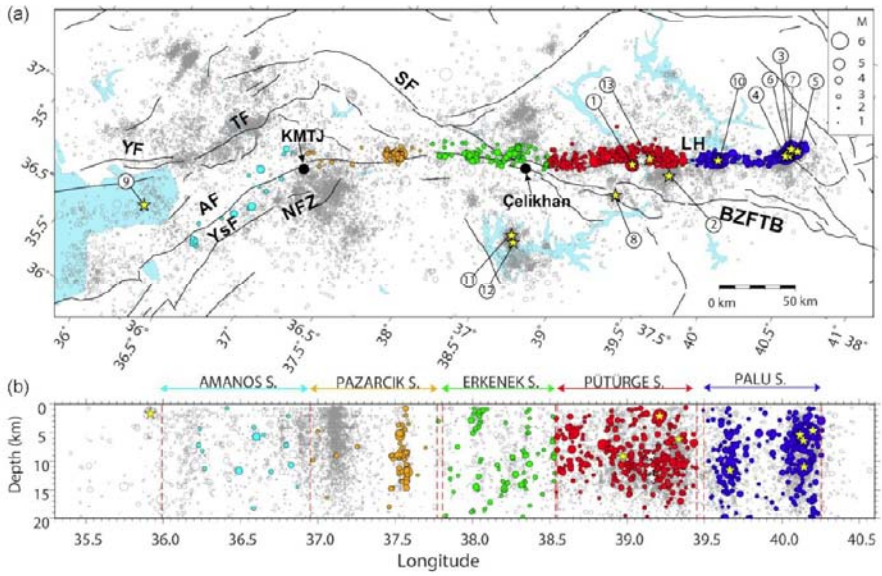

Figure 8: (**a**) Cartographic view and (**b**) seismicity depth section along the East Anatolian Fault for the period 2007–2019. Earthquakes with a magnitude greater than 2.5 are shown with colored circles according to the segments. Seismicity was taken into account within 15 on both sides of the fault axis. Numbers denote events with a magnitude greater than 5.0. KMTJ, Kahramanmarash node; LH, Lake Khazar; BZFTB, Bitlis-Zagros belt; SF, Syorgyu fault; AF, Amanos fault; YsF, Esemek fault; YF, Yumurtalyk fault; TF, Toprakkale fault; NFZ - Narla Fault [12].

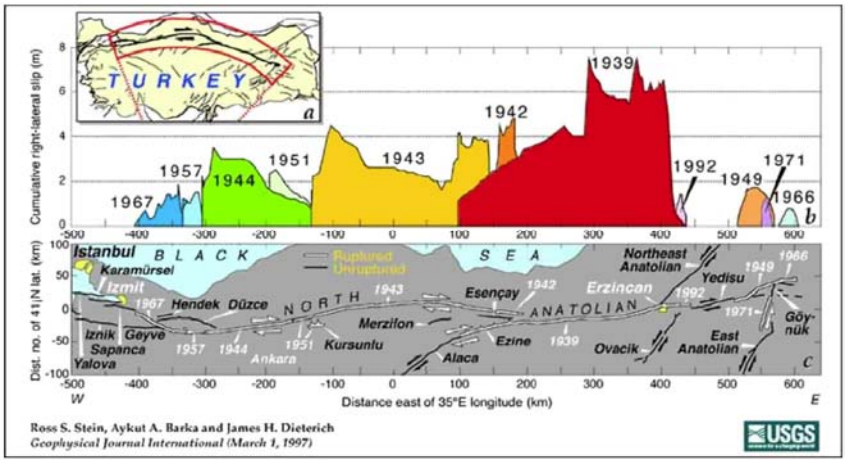

Figure 9: (a) Active faults in Turkey (Barka, 1992; Saroglu & Kusçu, 1992; Sengor, *et al.*, 1985), with the North Anatolian fault in bold. GPS observations establish a 24±4 mm/yr deep slip rate on the North Anatolian fault.

(b) Cumulative right-lateral slip associated with M>=6.7 earthquakes (Barka, 1995; Barka & Eyidogan, 1993; Bennett, *et al.*, 1996); the sequence ruptured from warm to cool colors. Slip in the 1949, 1966, and 1971 shocks is approximate.

(c) The region inscribed by the solid red line in *a* is projected relative to the Anatolia-Eurasia rotation pole, so that a transform fault would strike due east-west; the North Anatolian fault is seen to deviate less than 40 km from being a simple right-lateral transform [29].

occur along it, and activity gradually shifts further and further west into the Sea of Marmara, towards Istanbul. The segment of this zone adjacent to the city has not been activated for 250 years, and this gives 2 options for the development of events. In the first case, there is a constant and low-amplitude sliding of the plates relative to each other and the tectonic stress is removed in the form of a "silent earthquake". In the second case the absence of slip means the accumulation of stress in the fault zone, which, when it reaches a critical value, can be released by a sharp shock of enormous force. And that spells imminent disaster for Istanbul, a city of 14 million people. This is why studying and monitoring the state of the NAFZ is truly vital for Turkey.

10 years ago, work began on the project to create a Deep Geophysical Observatory on the North Anatolian

Fault (GONAF) of the International Continental Scientific Drilling Program (ICDP). These studies are carried out jointly by Turkish and German scientists. To monitor the seismic state of the NAFZ in the land areas closest to the main branch of the fault, the islands of Yassyada and Sivriada of the Princes' Islands of the Sea of Marmara, seismic stations are installed in wells up to 500 m deep, constantly monitoring microshocks along the dangerous segment with high resolution (Figure **10**).

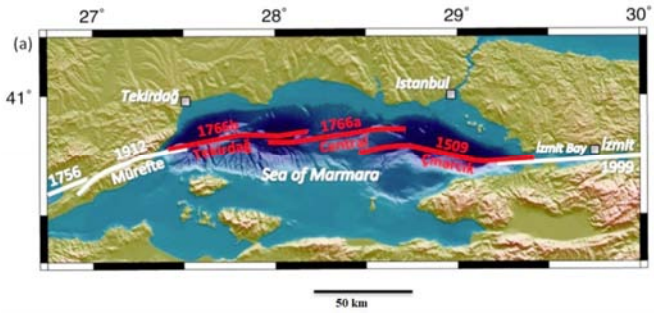

Figure 10: Red line - the Sea of Marmara segment, inactive since 1766.

http://www.gonaf.de/content/project/index.html

Also an international group of scientists from France and Germany undertook to study the underwater part of the NAFZ segment, located a few dozen kilometers from Istanbul. For this, a network of 10 transponders was installed at the bottom of the Marmara Sea in October 2014 (Figure **11**).

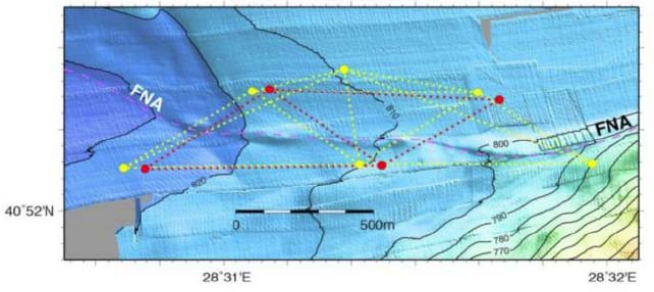

Figure 11: Network of acoustic transponders (red - German, yellow French), located on both sides of the North Anatolian Fault.

https://www.sciencedaily.com/releases/2016/07/160713115102.htm

The data obtained show that there are no significant movements along the fault within the resolution of the system. The distance between transponders located at a distance of 350 to 1,700 meters from each other is measured with a resolution of 1.5–2 mm. Based on the data obtained, scientists came to the preliminary conclusion that the segment is blocked or almost blocked and accumulates stress that can cause an earthquake. In combination with other types of monitoring, such work makes it possible to create a more complete and comprehensive picture of what is happening in this seismically hazardous region.

4. THE GEODYNAMIC MODELS OF NATURAL HAZARDS REGIONS

Geological-geophysical and seismic tomography research give possibility to connect complicated geodynamics and stress-strain state of the region with upwelling of mantle flow from the core boundary (Figures **12**, **13**).

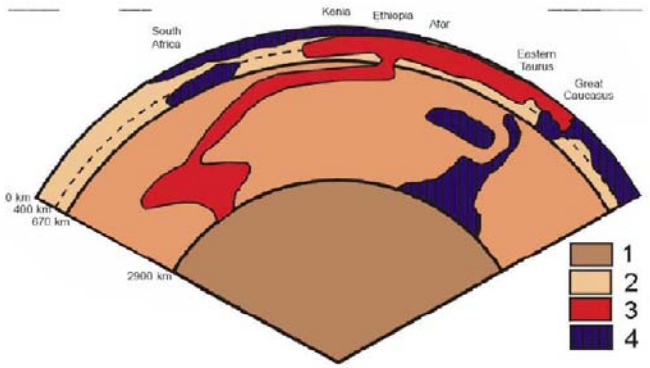

Figure 12: Schematic seismotomographic section across the mantle along 120° segment of the great circle passing through the point with coordinates 0° N and 35° E at azimuth 10°, (1) the Earth core; (2) mantle; (3) hot low-velocity zones; (4) cold high-velocity zones [6, 7, 45, 46].

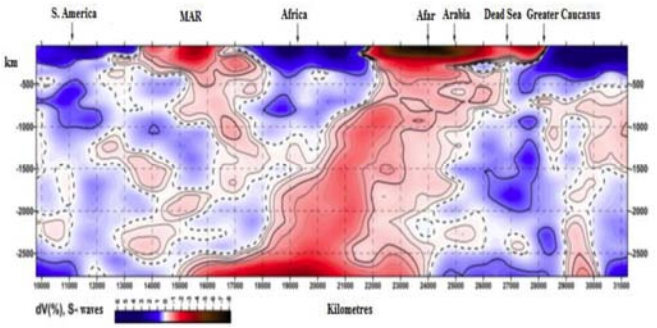

Figure 13: Section δV of NGRAND seismic tomographic model based on *S*-waves from mantle roof to its base from western coast of South America across Atlantic Ocean, Africa, and Arabia to East European Platform. Zero isoline is shown by dotted line [5, 11].

This upwelling of huge mantle flow is confirmed by magmatism and basalt volcanism (Figures **14-16**).

The origin and evolution of geological structures could be a clue for understanding the crust-mantle interaction. For a simulation of the evolution of geological processes and geological structures in

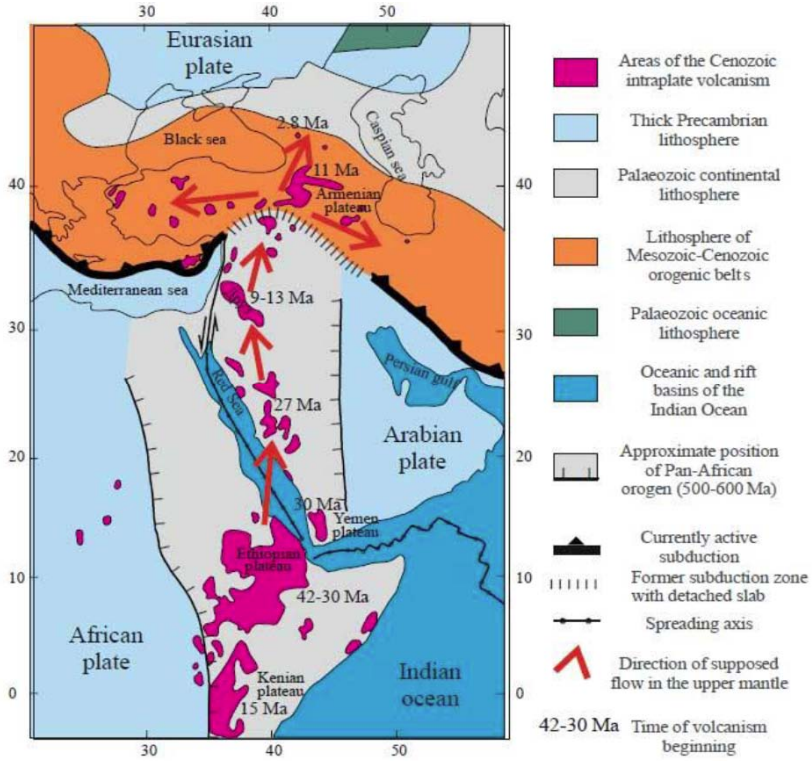

Figure 14: Tectonic units and distribution of Cenozoic intraplate plateau basalt volcanism and its ages. Numbers near volcanic plateaus designate their age, Ma [6].

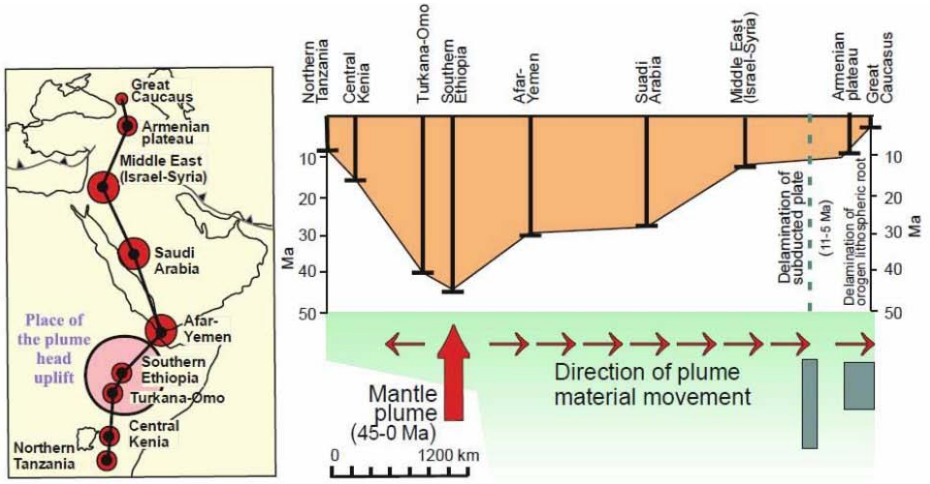

Figure 15: Age of volcanic activity versus distance along the hot belt [6].

connection with deep mantle movements, all possible geological-geophysical data were combined and analysed and the mechanical-mathematical models were used. In making analytical decision, it is possible to find the critical parameters of the problem. After defining boundary conditions on the uppermost surface, it is possible to make some conclusions about deep movements in the lithosphere [25, 34, 35, 38, 44].

One of the most interesting problems arising in the mechanical-mathematical modelling of the formation and evolution of geological structures is the description of matter behaviour above a rising mantle plume and a mantle diapir. A super plume is associated with super structures, such as continents and oceans. A diapir is responsible for geological structures, such as basins, orogenes and others [9, 10, 14, 25-27, 36-41, 44].

During many years of geological modelling, many interesting problems were solved. But the interest in superplumes, plumes and diapir modelling only increases.

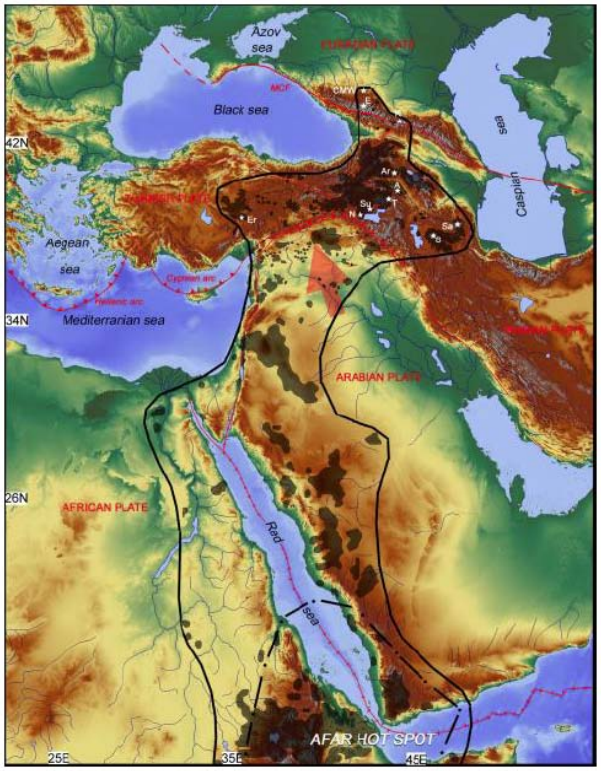

Figure 16: Distribution of the modern plume-related volcanism in the Afro-Arabian LIP (lithosphere plate) up to the Greater Caucasus. Black line – contour of projection of proposed mantle plume head to the surface. The fields painted by black represent the areas of young volcanic activity.

The largest Quaternary volcanoes: A - Ararat, Ar - Aragats, CMW - Caucasian Mineral Waters, E - Elbrus, Er - Ercies, K - Kazbek, N - Nemrut, S - Savalan, Sa - Sahand, Su - Suphan, T - Tendürek [23, 24].

One of the reasons is that mantle upwelling is associated with tectono-magmatic activization and the geothermal regime of the lithosphere.

The problem of the relationship between heat flow and the age of the last tectonic event is not solved yet.

Additional stimuli for the investigation of diapirs is the development of seismotomography. The possibility to ”see” a mantle plume increases the pressure to research different geological structures connected with plumes [14, 17, 22].

5. GEODYNAMICS OF THE CAUCASUS REGION

Analysis of geological and geophysical data on the development of the Caucasus region within the Alpine-Himalayan belt leads to the conclusion that the Caucasus can be considered as one of the most stressed and geodynamically active segments of the global structure, characterized by increased heat flow, high seismicity, magmatism and volcanism [9, 20, 41, 43].

From the point of view of deep geodynamics, the Caucasus is one of the most active zones of collision of lithospheric plates, characterized by significant speeds of horizontal and vertical movements (Figure **17**) [9, 43].

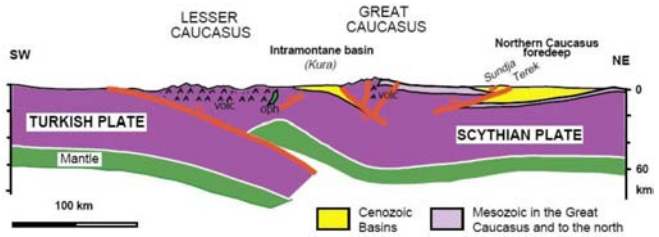

Figure 17: Schematic cross section through Caucasus [9].

The velocity field of the North Caucasus is characterized by horizontal displacement in the northeast direction at a speed of 26–28 mm / year. Relatively motionless Eurasia, a general compression of the region was revealed at a speed of 1–2 mm / year, which is the source of modern geological and seismic activity in the border region of the Caucasus and the East European platform.

Modern vertical movements of the North Caucasus region are characterized by small vertical movements of 2.5 mm / year in the lowland of Ossetia, the highest ascent rates for the region of about 3.5–4.5 mm / year in the mountainous part of the North Caucasus, and moderate steady rise of 2.9 mm / year in the northern part of the northern slope of Greater Caucasus [20] (Figures **18**, **19**).

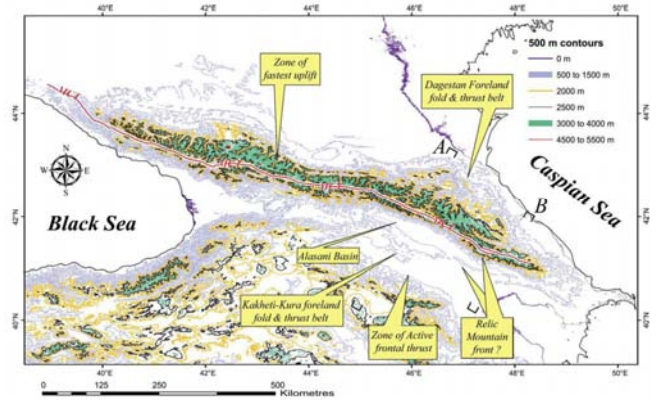

Figure 18: Caucasus faults and topography map. The zone of highest topography (green colour) and zone of fastest uplift (Jon Mosar *et al.*, 2010).

According to geodynamic ideas, on the site of the Greater Caucasus 35 million years ago there was a

deep-water basin about 200 km wide. With the gradual closure of its sides, they approached until a complete collision about 11 million years ago, after which the region began a constant uplift. During compression, the lithosphere material formed a mountain belt with a crust thickness of 45-50 km and a lithosphere thickness of up to 250 km. Later, 5–10 million years ago, the Greater Caucasus began to rise rapidly, and volcanoes Elbrus, Kazbek, and others arose on its axis [14]. Apparently, this is due to the rise of the asthenosphere due to compression and gravitational instability.

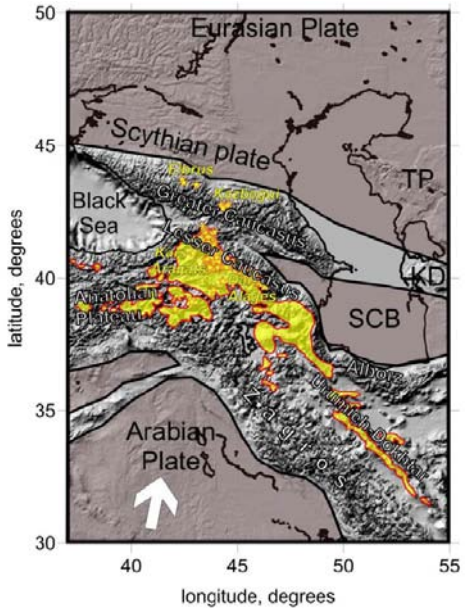

Figure 19: Main tectonic units in Caucasus and surrounding areas. Yellow stars - the recent volcanoes in Caucasus.

TP - Turan Plate; KD - Kopeth-Dagh; SCB - South Caspian Basin. White arrow - the direction of the Arabian Plate displacement [17].

The structure of the Alpine zone includes individual sea depressions, sedimentary basins and mountain formations. Above the rising mantle diapirs on the Earth's surface, the structures of the arched uplift, sedimentary basin, or the outflow of basalts can form, depending on the stage of diapir uplift and its energy [25, 34, 35, 38, 44]. At the same time, compression zones are formed between the individual diapirs, leading to mountain building and thickening of the crust. So the depressions of the western sector of the Alpine-Himalayan belt (Alboran, Balearic, Tyrrhenian, Ligurian, Pannonian, Ionian, Black Sea, Pre-Caspian Depression, Middle and South Caspian) can be associated with rising mantle diapirs, and the Caucasus not only with the zone of collision of lithospheric plates but also with the zone of collision of lithosphere flows from two mantle diapirs beneath the hollows of the Black and Caspian Seas.

The complex stress-strain state of the lithosphere of the Caucasus is expressed in the presence of faults, fracturing of rocks, manifestation of magmatism and volcanism, high seismicity, increased heat flow, hydrothermal activity, and is also confirmed by seismic data and seismotomography.

6. GEOTHERMY OF THE CAUCASUS REGION

The value of the heat flux density is an indicator of the geodynamic activity of the structures of the lithosphere. Comparison of the heat flux density with the thickness of the Earth's crust gives mixed results. For individual blocks of the cortex, there is a direct connection of these parameters, for others, the inverse one. Feedback is more common when a thin crust corresponds to a high heat flux. This is explained by the removal of deep heat by the mantle diapir with the formation of a zone of extension and thinning of the crust. An example of a direct connection is the basin of the Black Sea with a thin earth crust. In this structure, low values of the heat flux (30–40 mW / m 2) with a low power of the Earth's crust are noted. [6, 19]. This may be explained by avalanche sedimentation and the more complex geodynamics of the structure.

Another situation with a high heat flux is observed in orogenic regions with a thick crust, for example, in the Himalayas, meganticlinoria of the Greater Caucasus, etc. The high heat flux here is due to the high geodynamic activity of the asthenosphere, manifested by magmatism and geothermal activity.

The Caucasus region is characterized by a complex and highly differentiated thermal field. Reduced flows correspond to foothill and intermountain troughs, elevated folded zones. The average heat flux for the folded region of the Caucasus is 78 mW/m^2 [21 42].

The nature of the thermal field of the Caucasus region correlates well with the features of its geological structure and development history. Zones of folding and manifestations of young volcanism are distinguished by high heat fluxes. Piedmont and intermountain troughs correspond mainly to low heat fluxes. The structure of the sedimentary cover and the structure of the foundation have a significant effect on the nature of the thermal field.

7. DESCRIPTION OF THE MODEL

For simulation of the formation and evolution of geological structures, a roof and base surface of the

lithosphere can be considered as the top and bottom boundaries of the simulation, where the boundary and initial conditions of a problem depend on a particular statement. Boundary conditions on the uppermost surface are much more reliable owing to the greater security of an authentic geological-geophysical material. The system JPS gives the information on the surface motion. The geologic data make an invaluable contribution to the representation of the relief motion.

The geothermal, geomagnetic, and gravitational fields give additional information about the formulation of boundary conditions on the Earth's surface. On one hand, the internal seismic boundaries in the stratified lithosphere monitor reference marks of simulation, and on the other hand, these boundaries are the outcome of simulation, when the suppositions about the previous system conditions result in a modern picture of a geologic pattern with the applicable geophysical fields.

The solution of inverse problem of geophysics, as it is known, is ill-defined problem. The forecasting of the internal constitution and plutonic characteristics of shells of the planet under the geophysical surface data is a complicated mathematical problem, influenced by the approach of different authors. The mechanical behaviour and transformation of matter at depth fundamentally determines the surface structure of geophysical fields.

So the rise of the molten mantle diapir, achievement of a level of buoyancy, and the cooling and crystallization of matter change temperatures, gravitational and magnetic fields. An analysis of the legitimacy of such connections is an indispensable stage of the geological-geophysical data and the outcomes of simulation. In this way, special concerns introduce the solution of an inverse geodynamical problem when under the geological-geophysical data on a surface it is possible to forecast the behaviour of matter at depth.

There are two standard ways to solve inverse problems – the regularization method, when the parameters of the solution of specific limitations are superimposed, and the approach method, when an inverse problem is decided by the solution of many direct problems.

The most interesting feature is the capability of the direct method to solve inverse problems of geodynamics when using reliable geological-geophysical surface data enables us to forecast behaviour of matter at depth in a unique manner.

An important technique applied in the studies of geological structures at different phases of evolution and analysis of velocity fields, stresses and temperatures in the sedimentary cover, crust and upper mantle in different tectonic environment is the construction of an adequate mechanical-mathematical model of the geological region evolution.

In order to get approximation system of mechanical equations by means of analyzing order of respective values in these equations it is anavoidable to separate small parameters of the problem which can be used for the decomposition.

Let us consider the behaviour of a layer of high-viscosity, incompressible fluid describing behaviour of matter of the lithosphere [8, 11, 12, 15, 21]. Let us the characteristic size of modelled patterns on lateral L considerably surpasses characteristic thickness of the layer h.

Numerous geological structures are characterized by rather gentle occurrence of layers and significant elevation of horizontal regional scale L over vertical scale h of typical thickness. This allows to introduce small parameter h/L into analysis of the problem. The second small parameter of the problem F/R, F – Froude number, R – Reynolds number, arises while analyzing rheological behavior of matter in the layers [8, 11, 12, 15, 21].

Slow lithospheric deformations will be simulated by models of viscous flow in multi-layered, incompressible, high-viscosity Newtonian fluid, using Navier-Stocks equation and discontinuity equation (1):

$$d\mathbf{v}/dt = \mathbf{F} - (1/\rho)\text{grad } p + (\mu/\rho)\Delta\mathbf{v} \quad (1)$$

$$\text{div } \mathbf{v} = 0$$

v – velocity vector, **F** – force of gravity, p – pressure, ρ – density, μ - viscosity, t - time.

Let us introduce dimensionless values for coordinates, velocities and pressure X, Y, Z, U, V, W, P:

$x=LX$, $y=LY$, $z=hZ$, $u=u_0U$, $v=u_0V$, $w=u_0(h/L)W$, $p=\rho_0 ghP$.

ρ_0 , u_0 - characteristic scales of density and velocity.

Then using an equation of continuity and an approximated equation of the Navier-Stockes for enough slow motions in a thin layer, it is possible to obtain in a dimensionless form for a two-dimensional case [8, 11, 12, 15, 21]:

$$\begin{cases} \dfrac{\partial P}{\partial X} = \alpha\mu \dfrac{\partial^2 U}{\partial Z^2} \\ \dfrac{\partial P}{\partial Z} = -\rho \end{cases} \quad (2)$$

$$\frac{\partial U}{\partial X} + \frac{\partial W}{\partial Z} = 0$$

$$\alpha = \frac{F}{R\left(\dfrac{h}{L}\right)^3}\ ,\ F = \frac{{u_0}^2}{gL}\ ,\ R = \frac{u_0 L \rho_0}{\mu_0} \quad (3)$$

Here P is pressure, U,W – velocities, F - Froude number, R – Reynolds number, ρ - density, μ - viscosity, ρ_0, μ_0, u_0 - scales of density, viscosity and velocity.

The forces on the high boundary are equal zero (free surface). Let the velocities U^*, W^* on the high boundary of simulation ς^* are known. Then it is possible to find the velocity distribution and pressure in the layer:

$$P = \rho\left(\varsigma^* - Z\right) \quad (4)$$

$$U = U^* + \frac{\rho}{2\alpha\mu}\frac{\partial \varsigma^*}{\partial X}\left(\varsigma^* - Z\right)^2 \quad (5)$$

$$W = W^* + \frac{\partial U^*}{\partial X}\left(\varsigma^* - Z\right) + \frac{\rho}{2\alpha\mu} \left[\frac{\partial^2 \varsigma^*}{\partial X^2}\frac{1}{3}\left(\varsigma^* - Z\right)^3 + \left(\frac{\partial \varsigma^*}{\partial X}\right)^2\left(\varsigma^* - Z\right)^2\right] \quad (6)$$

On the high boundary, the kinematic condition of a free surface should also be executed. This means that points of a surface will not escape it during motion:

$$S\frac{\partial \varsigma^*}{\partial t} + U^*\frac{\partial \varsigma^*}{\partial X} - W^* = 0 \quad (7)$$

$$S = \frac{L}{u_0 t_0} \quad (8)$$

Here S is the Strukhal number. t_0 is the scale of time.

Similarly it is possible to consider the lower boundary of simulation as a surface where the points remain during the evolutionary process (the condition of non-penetration). Then, substituting velocities, we get an equation of movement for the lower boundary ς_*:

$$S\frac{\partial \varsigma_*}{\partial t} - W^* + U^*\frac{\partial \varsigma_*}{\partial X}\left(\varsigma^* - \varsigma_*\right) + \frac{\rho}{2\alpha\mu}\left[\frac{\partial \varsigma_*}{\partial X}\frac{\partial \varsigma^*}{\partial X}\left(\varsigma^* - \varsigma_*\right)^2 - \frac{\partial^2 \varsigma^*}{\partial X^2}\frac{1}{3}\left(\varsigma^* - \varsigma_*\right)^3 - \left(\frac{\partial \varsigma^*}{\partial X}\right)^2\left(\varsigma^* - \varsigma_*\right)^2\right] = 0 \quad (9)$$

The given equation represents the direct solution of an inverse problem when a relief of the uppermost surface and velocities on it determine the geodynamics of the deep boundaries. A similar equation can be written for any material boundary at depth through which the flow of matter is absent.

8. THE ANALYSIS OF THE OBTAINED SOLUTION

Thus, setting the motion of the upper surface, we have an equation of motion for the deep boundaries.

Some conclusions about the structure of deep motion on known speeds and relief of a surface can be made by analysing the velocity distribution at depth.

Let us consider some typical cases of formation and evolution of the geological structures.

Case 1. Sedimentary Basin Under Stretching Surface Conditions

Uppermost surface is concave, that is $\frac{\partial^2 \varsigma^*}{\partial X^2} > 0$.

Sgn U* = Sgn X

Analysis shows that U increases with depth and with gradς^*.

W describes rising flux at depth.

Case 2. Sedimentary Basin Under Pressing Surface Conditions

Uppermost surface is concave, that is $\frac{\partial^2 \varsigma^*}{\partial X^2} > 0$.

Sgn U* = - Sgn X.

Analysis shows that critical depth exists where horizontal pressing is changed by stretching:

$$\varsigma_* = \varsigma^* - \sqrt{-\frac{U^*}{\dfrac{\rho}{2\alpha\mu}\dfrac{\partial \varsigma^*}{\partial X}}} \quad (10)$$

W can be positive or negative, depending on the relationship between task parameters. But in the center of the structure, W is positive (uprising).

In a stretching basin, the uprising flux at depth is more intensive.

Case 3. Orogene Under Stretching

Uppermost surface is convex, that is $\frac{\partial^2 \varsigma^*}{\partial X^2} < 0$.

Sgn U* = Sgn X.

Hence, a critical depth exists where stretching is changed by pressure:

$$\varsigma_* = \varsigma^* - \sqrt{-\frac{U^*}{\frac{\rho}{2\alpha\mu}\frac{\partial \varsigma^*}{\partial X}}} \quad (11)$$

Analysis of W shows descending flux in the center of the structure at depth.

If stretching is intensive, the uprising flux can exist.

Case 4. Orogene Under Pressure

Uppermost surface is convex, that is $\frac{\partial^2 \varsigma^*}{\partial X^2} < 0$.

Sgn U* = - Sgn X.

In this case, pressure is in whole layer. Descending flux at depth exists with high probability.

Preliminary analysis shows that a stretching basin and an orogene under pressure are more stable structures than basin under pressure and orogene undergoing stretching.

It is possible to forecast deep movements in the lithosphere if the geodynamics of the uppermost surface are known. Complex interpretation of geological-geophysical data, together with mechanical-mathematical modelling, are effective instrument to explain the evolution of geological structure.

The collision of lithospheric plates is determined by the collision of deep asthenospheric flows. Plates move due to movements in the asthenosphere. The geodynamics of the collision zone of asthenospheric flows is determined by the ratio of the density, viscosity, and temperature of the layers of the lithosphere and asthenosphere. The same relations determine how intensively the lithosphere plate overlaps the rise of the asthenosphere and how fast the asthenosphere diapir rises in the collision zone, forming the structure of back-arc spreading or thickening of the asthenosphere and rise of the lithosphere. The complex geodynamic picture is determined by the ratio of geological and geophysical parameters and external limiting factors for speeds and motions on the spherical surface of the Earth and in its depths.

So, based on the analysis of the obtained relations for surface movements, we can speak of the presence of downward movements in the lithosphere with the immersion of the bottom of the lithosphere under mountain structures, which can be the case in the Caucasus.

Thus, in the Caucasus region, at the bottom of the lithosphere, downward flows of matter and subsidence of the lithosphere must exist (Figure **20**).

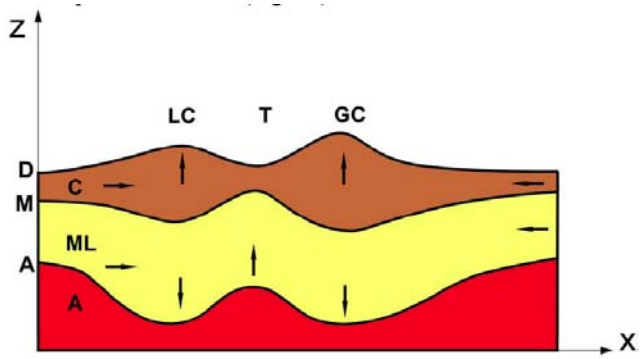

Figure 20: Schematic cross-section of the Caucasus region on the base of mechanical-mathematical modeling.

D – upper surface, M – Moho boundary, A –asthenosphere surface, C – crust, ML – mantle lithosphere, LC- Lesser Caucasus, GC - Great Caucasus, T - Caucasus Trough. Arrows – possible directions of the matter movements.

It is interesting to compare the results of mechanical-mathematical modeling with the data of geological and geodynamic reconstruction and seismotomography (Figure **21**) [17].

Solution of the inverse problem of geodynamics by the direct method is proposed and developed. The first inverse problem of geodynamics is solved - the restoration of the velocity, pressure and stress fields at the depth of the lithosphere from the available data on the velocities on the day surface. The second inverse problem of geodynamics is posed and solved - the determination of the movement of boundaries at the depth of the lithosphere by the given movements of the

day surface. The obtained solutions can be used to analyze deep geodynamic problems, and together with geothermal modeling, geological and geophysical methods and seismotomography can serve as a reliable tool for studying the deep geodynamics of geological structures and forecasting oil and gas potential.

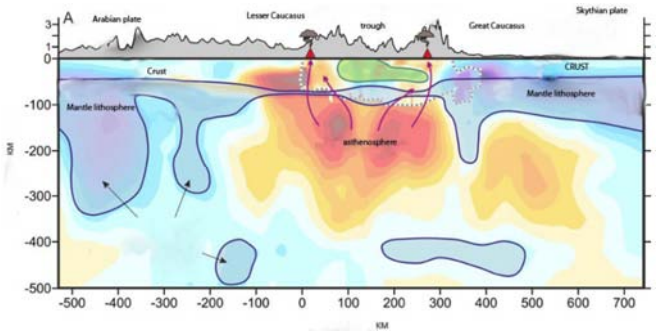

Figure 21: Seismotomographic cross-section of the Caucasus region.

Lesser Caucasus, Great Caucasus, Caucasus Trough.

Red and yellow – asthenosphere, dark blue – mantle lithosphere, light blue – crust, green – higher density crust [17].

It should be understood that geophysics and seismotomography give a deep section at present time, while mechanical and mathematical modeling allows us to study the evolution of the structure in dynamics. A comparative analysis of various approaches and solutions makes it possible to more reliably draw conclusions about the underlying mechanisms of movements and their manifestation on the Earth's surface and substantiate the most probable reasons for the formation and evolution of various geological structures and processes.

Similar model as for Caucasus can be applied to all region of Arabian-Caucasus region that demands detailed collection of surface velocities.

9. DISCUSSION

As earthquakes are so widespread, earthquake mechanisms would seem to be an indicator of stress in the crust. There is important information about stress magnitudes and relative orientations in focal mechanism observations [47, 48]. These data interpretation is very important (Figure **22**).

Surface velocities must be analyzed from different sources [30]. But for purposes of mechanical-mathematical modeling the vertical and horizontal velocities must be evaluated in details and in big scale depending on modeling region (Figure **23**).

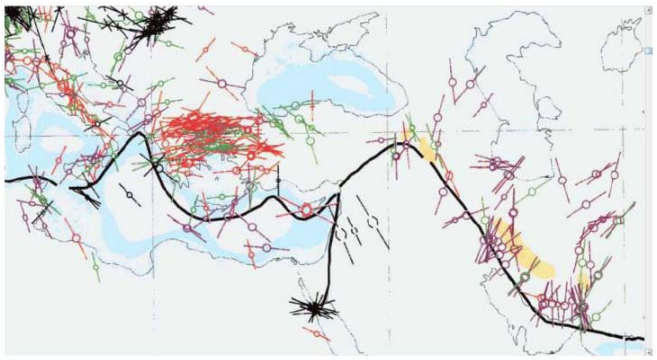

Figure 22: Generalized world stress map (detail). Inward pointing arrows indicate high compression. Paired inward and outward arrows indicate strike-slip faulting. Outward directed red arrows indicate areas of extension. The plates are generally in compression and the areas of extension are limited to thermally uplifted areas [47, 48].

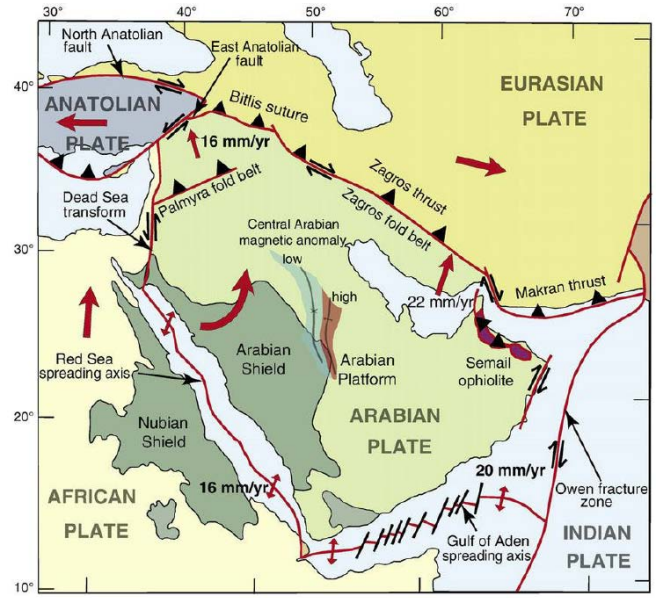

Figure 23: Simplified map of the Arabian Plate, with plate boundaries, approximate plate convergence vectors, and principal geologic features. Note location of Central Arabian Magnetic Anomaly (CAMA) [30].

Seismotomographic data confirm the existence of a lithospheric window beneath eastern Anatolia, through which hot material of the asthenosphere rises, and this help clarify the deep structure under eastern Anatolia [18, 19] (Figure **24**).

In the Bitlis zone depth of Moho is 42 km, and in the northern part, under the largest in the region North Anatolian fault, the depth of the Moho border reaches 50 km.

This could be a reason for different frequency of large earthquakes along North Anatolian and East Anatolian faults. Thick crust along North Anatolian fault is broken

every 1-10 years (1939, 1942, 1943, 1944, 1953, 1957, 1966, 1967, 1971, 1992, 1999) with distance between hypocenters near 100 km with direction to the west (Figure **9**, **28**).

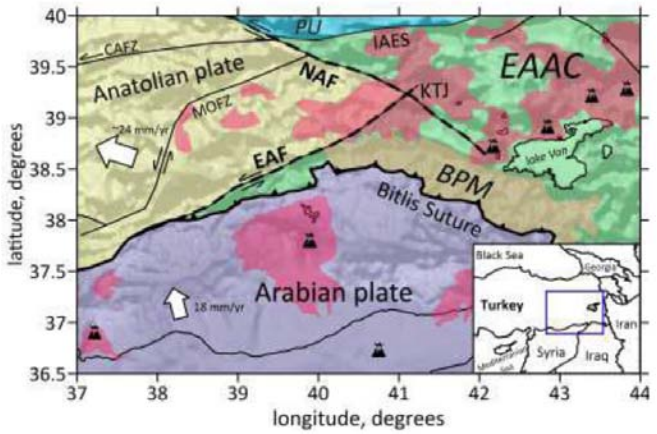

Figure 24: The simplified regional tectonic map of Eastern Turkey with topographic relief Pink areas are Neogene–Quaternary volcanism. Arrows indicate the direction of plate and fault motions. BPM – Bitlis-Poturge Massif; CAFZ – Central Anatolia Fault Zone; EAAC—East Anatolian Accretionary Complex; EAF—East Anatolian Fault; IAES – Izmir-Ankara-Erzincan Suture; KTJ—Karlova Triple Junction; MOFZ—Malatya-Ovacik Fault Zone; NAF—North Anatolian Fault; PU—Pontide Unit [18, 19].

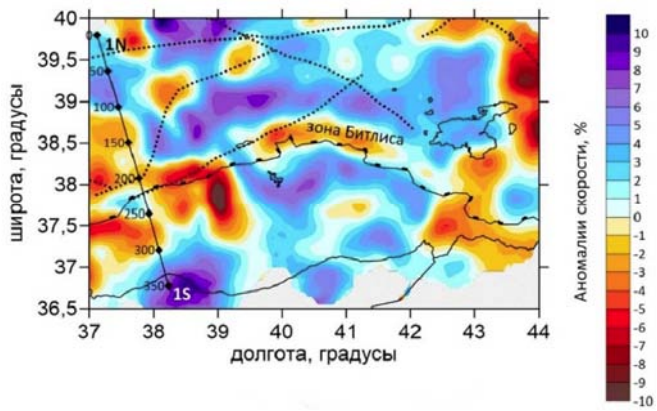

a

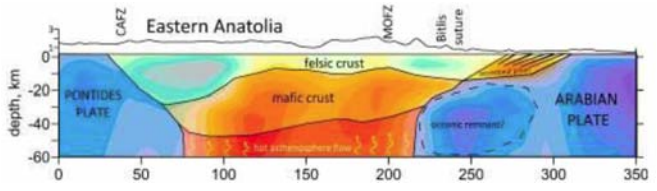

b

Figure 25: a. Horizontal section of P-velocity anomalies at a depth of 50 km. latitude, degrees (left); longitude, degrees (below); Bitlis zone (center); speed anomalies (right) [18, 19].

b. Scheme of the Crustal Structure along profile 1N -1S (a) under Eastern Anatolia [18, 19].

As Izmit earthquake of 1999 was in 80 km east of Istanbul, it is possible to wait earthquake near Istambul in some years (1-10 years).

As East Anatolian fault produced large earthquakes in 1789 (M 7.2), 1795 (M 7.0), 1872 (M 7.2), 1874 (M 7.1), 1875 (M 6.7), 1893 (M 7.1), 2020 (M 6.8), 2023 (M 7.8, M 7.7), it means the frequency of groups (1790 – 1880 – 2020) near 100 years. But inside the groups there are 2-4 close in time large earthquakes. It could reflect matter rheology and lithosphere geodynamics of the region. Now it is necessary to understand and investigate if 3 last large earthquakes of 2020 and 2023 (2) produced enough relaxation of material or not. And we must wait the next large earthquake there soon (near 1-2 years). As there were many aftershocks after 2023 earthquakes and they continue, maybe the next large earthquake there will be not so soon but in 100 years only. It is possible to forecast that if large earthquake in Earst Anatolian fault will not occur in 1-2 years, it will happen in 100 years.

It is necessary to understand that collision zone is very complicated one. And the lithosphere behavior there can be imagine and analyzed only schematically (Figure **26**).

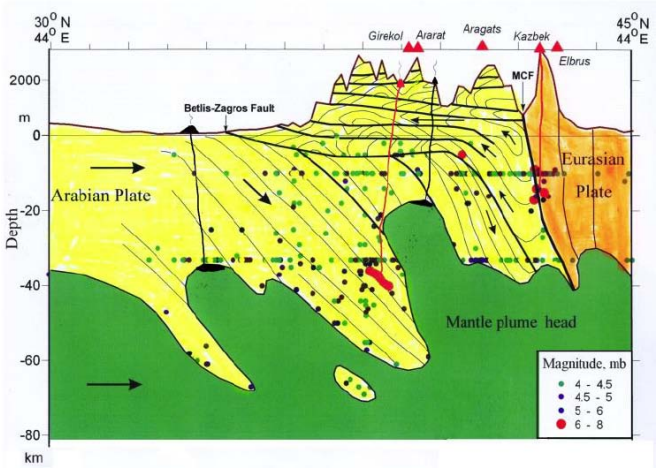

Figure 26: Schematic structure of zone of Arabian-Eurasian convergence and magma-forming processes beneath it [23, 24].

It is known which tectonic processes lead to earthquakes and how often they occurred in the past. Long-term forecasts, which operate with intervals of tens and hundreds of years, are possible based on both the seismic history and the seismicity of the region. If somewhere once there was an earthquake of great magnitude, it is logical to assume that it can happen again.

The physical expression of such a forecast is seismic zoning maps, which indicate how often earthquakes occur in the region and what intensity they reach. They are regularly updated in accordance with the latest seismic monitoring data. Based on these maps, seismic stability standards for buildings and structures are developed [32, 33].

Medium-term forecasts predict which earthquakes can occur in the interval from a year to a decade. But their accuracy is not very great.

For the medium-term forecast, the M8.0 algorithm was used, which should predict earthquakes of magnitude 8 and above. This method has been developed since the 1990s. The input data is information about weaker earthquakes—their magnitude, frequency, recurrence, grouping in time, and other characteristics—in a zone about 800 kilometers in diameter [13,16].

The practical value has a short-term forecast - for a period from a month to a year. There is no reliable method for it yet.

For a short-term forecast, additional geophysical data are involved, which could serve as indicators of an approaching event, for example, anomalous disturbances in the atmosphere and ionosphere. Researchers are trying to improve the accuracy of medium-term forecasts based on the theory of lineaments by bringing them closer to short-term ones on a time scale.

Such indicators as fluctuations in the concentration of radon and helium, changes in the level of groundwater, their chemistry and isotopic composition, the occurrence of electromagnetic phenomena, and changes in the behavior of animals are involved. Important precursors are foreshocks, a change in the stress-formed state of the medium, fixed by a change in the velocities of the passage of seismic waves, and a change in the velocities of the surface. There is no universal precursor. It is necessary to analyze the entire complex of precursors. The forecast of a strong earthquake implies the need to evacuate the population and stop production, which entails economic damage and has a serious psychological impact on people. It's too big a responsibility.

The only successful attempt of this kind was the prediction of an earthquake of magnitude 7.3 in Haicheng (China) in 1975, when timely evacuation prevented the death of several hundred thousand people. The Haicheng earthquake was predicted by its precursors, in particular, by a strong shock, which was correctly qualified as a foreshock, an event that precedes the main seismic shock. As a rule, they are found retrospectively, after the main earthquake has already happened. But the very next year, the Tangshan earthquake, also in China, could not be predicted, and it killed more than 242,000 people.

Great progress has been made in the field of earthquake prediction based on the theory of block structures, which makes it possible to describe the real behavior and properties of the earth's crust with high accuracy. A geoinformation model "Seismozone" has been developed, which allows tracking the movement of stress concentration zones in the earth's crust, assessing the risks of earthquakes, predicting their strength, place and time. A system for geodynamic monitoring of the movement of lithospheric plates in the Black Sea region of the South of Russia has been created, studies have been carried out on the seismic safety of cities that are at the intersection of geophysics and mechanics, and a seismic safety system has been developed for the Sochi 2014 Olympics [2-4].

One of the fruitful approaches to the problem of earthquake hazard reduction, along with the development of earthquake-resistant construction, is the use of risk assessment and management methods. It is also important to single out the most dangerous regions according to the degree of risk in order to organize systems for monitoring and warning the population, for which the concept of risk “hot spots” is introduced [31].

"Hot spots" according to the degree of geoecological risk are a superposition of areas of maximum probability of a dangerous event and areas of maximum potential damage in case of an event.

Geoecological risk is considered as a probabilistic measure of danger. One of the most common definitions of geological risk is that risk is the mathematical expectation of damage. Or the risk is equal to the product of the probability of a possible dangerous event and the damage produced:

$$R = PxD$$

where R is the risk; P is the probability; D - damage.

Damage is meant both purely economic - to buildings and structures, and the damage expressed in money from the loss of human lives.

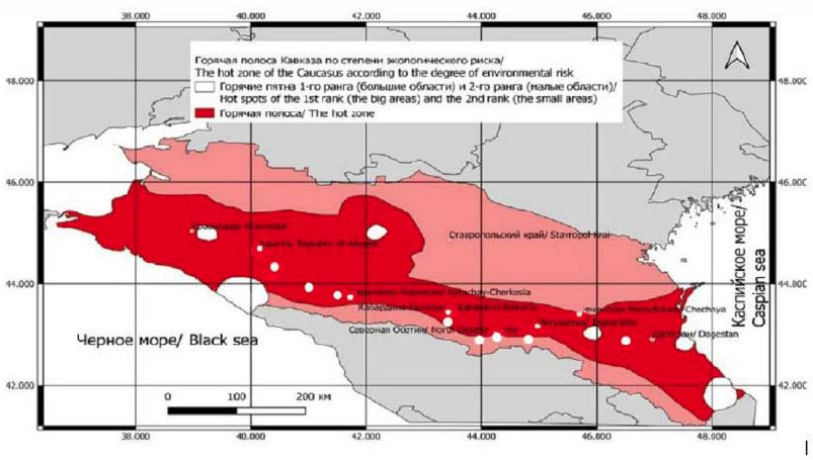

Figure 27: "Hot spots" of risk in the "hot zone" of the Caucasus (dark zone). Large white circles are "hot spots" of the 1st class, small white circles are of the 2nd class (Svalova, 2022).

By analyzing all the geological and geophysical data and parameters of potential damage to the Caucasus region, it is possible to identify and define the "hot zone" and "hot spots" of the Caucasus.

The "hot zone" of the Caucasus in terms of the degree of environmental risk, which characterizes the zone of collision of the African and Eurasian lithospheric plates, runs from Makhachkala through Grozny, Vladikavkaz and Krasnodar, expanding to the Black Sea coast of the Caucasus and the Sea of Azov. On the territory of the "hot zone" there are "hot spots" of the 1st risk class associated with a high population density and especially valuable objects - Derbent, the only UNESCO cultural heritage site in the Caucasus, and the Sochi mountain cluster with Olympic sites, as well as "hot spots » 2nd risk class - large cities and resorts of the North Caucasus [31].

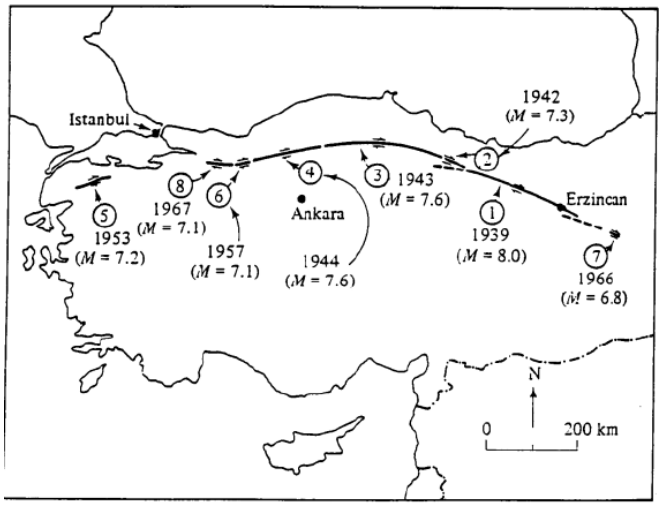

Figure 28: The North Anatolian fault and its associated strong earthquakes [1].

Similarly, for the entire Caucasus- Anatolian - Arabian region, the "hot spot" of risk is Istanbul, as well as other large cities along the North Anatolian fault, Western branch of the North Anatolian fault and East Anatolian fault (Figures **28**, **29**).

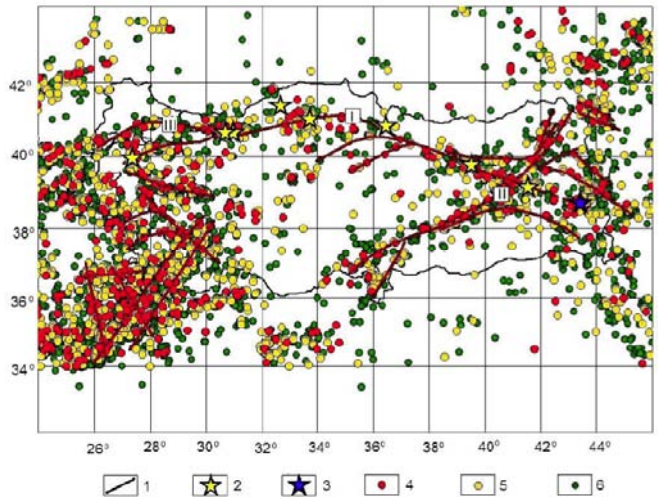

Figure 29: The main faults and earthquakes in Turkey.

1 – main faults: I – the North Anatolian fault, II – the East Anatolian fault, III – the Western branch of the North Anatolian fault; *2* – strong earthquakes; *3* – new events; *4–6* – earthquakes with magnitudes M: *4* – ≥5.4, *5* – 4.8–5.3, *6* – 4.3–4.7 [28].

10. CONCLUSIONS

The earthquakes prognosis and prediction is one of the most important task and problem of the modern geoscience and national economy in many countries, which is not decided yet (Figure **30**, **31**).

Map of active and seismogenic faults can be a clue for the problem decision (Figures **32**, **33**).

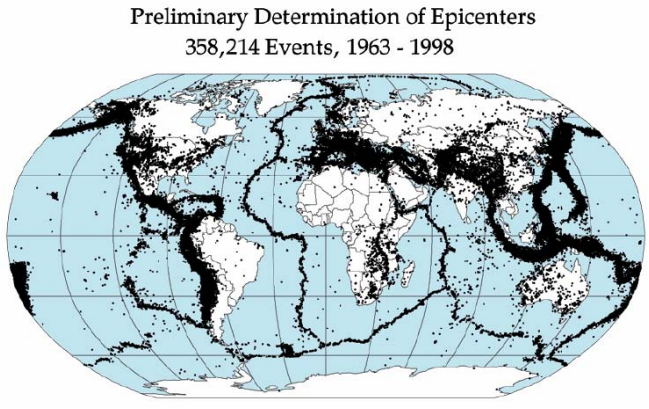

Figure 30: Epicenters of the earthquakes (1963—1998).

https://ru.wikipedia.org/wiki/Землетрясение#/media/Файл:Quake_epicenters_1963-98.png

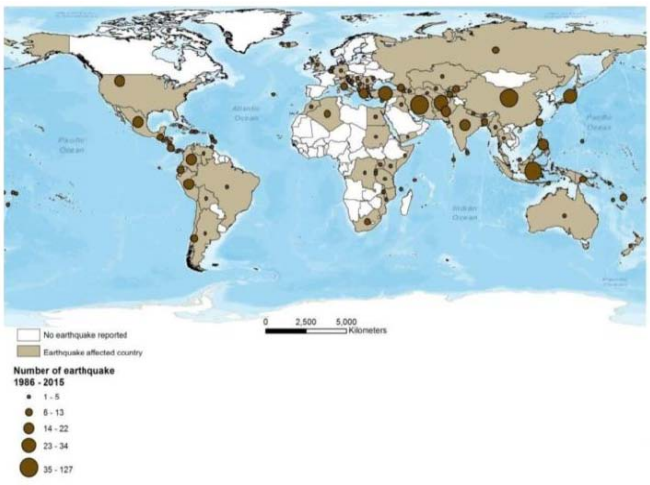

Figure 31: Number of earthquakes in 1986–2015 by country http://emdat.be/.

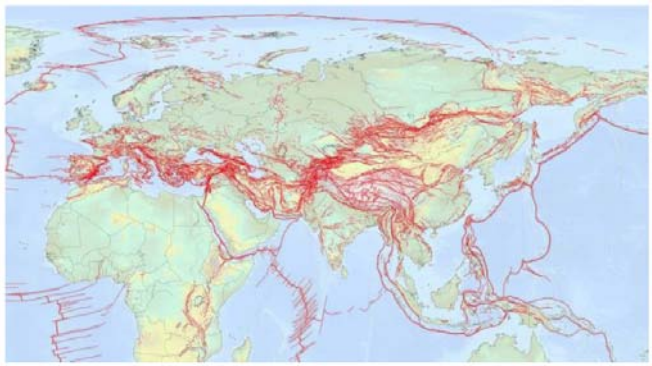

Figure 32: Map of active and seismogenic faults of Eurasia 2018 (neotec.ginras.ru)

Geodynamic model of the Caucasus- Anatolian-Arabian region is determined by huge mantle flow upwelling from the core surface and its spreading below lithosphere producing complicated surface velocities in Anatolia to the west, in Arabian plate to the east and in Caucasus to the north. This flow will continue to move matter along North Anatolian and East Anatolian faults.

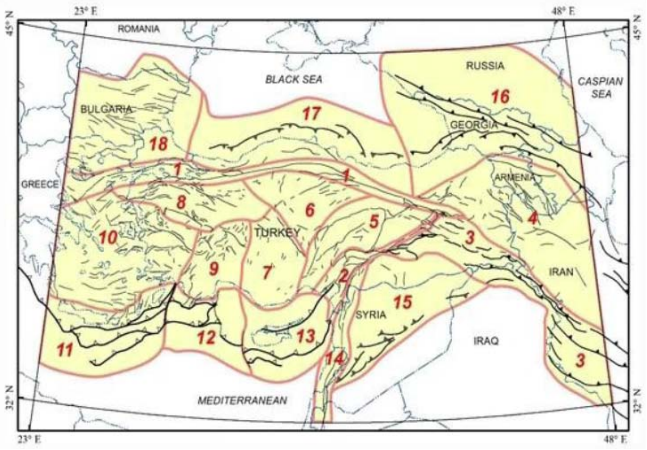

Figure 33: The main seismotectonic regions of Turkey and Caucasus, determined by the nature of seismicity and the presence of faults with similar characteristics [8].

There is different frequency of large earthquakes along North Anatolian and East Anatolian faults. Along North Anatolian fault large earthquakes occur every 1-10 years (1939, 1942, 1943, 1944, 1953, 1957, 1966, 1967, 1971, 1992, 1999) with distance between hypocenters near 100 km with direction to the west (Figure **34**).

As Izmit earthquake of 1999 was in 80 km east of Istanbul, it is possible to wait earthquake near Istambul in some years (1-10 years). Istanbul can be considered as “hot spot” of earthquake risk.

Area of highest seismicity in Turkey (red color in Figure **34**) can be considered as ”hot zone” of earthquakes danger and big towns there are “hot spots” of earthquake risk (Figure **34**). In any case it is necessary to check and strengthen buildings and constructions in the towns from “hot zone”.

As East Anatolian fault produced large earthquakes in 1789 (M 7.2), 1795 (M 7.0), 1872 (M 7.2), 1874 (M 7.1), 1875 (M 6.7), 1893 (M 7.1), 2020 (M 6.8), 2023 (M 7.8, M 7.7), it means the frequency of groups (1790 – 1880 – 2020) near 100 years. But inside the groups there are 2-4 close in time large earthquakes. As there were many aftershocks after 2023 earthquakes and they continue, the next large earthquake there will be in 100 years only. It is possible to forecast that if large earthquake in East Anatolian fault will not occur in 1-2 years, it will happen in 100 years only.

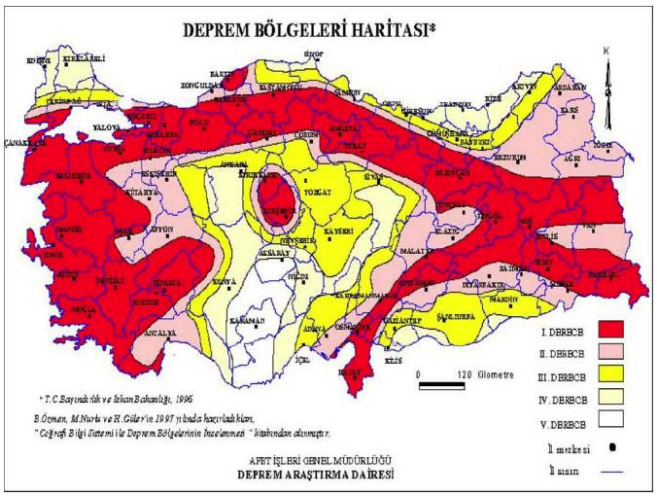

Figure 34: Istanbul as “hot spot” of earthquake risk (white sircle). “Hot zone” of earthquakes danger (red color) in Turkey. Basement: Earthquake zones map (Earthquake research department. General directorate of disaster affairs, Turkey).

The next steps and scheme is suggested for approach to the prognosis problem decision:

Concept and Algorithm of the Earthquakes Forecast, Prognosis, Prediction and Risk Reduction

1. To combine all possible geological-geophysical, seismotomographic and precursors data in the region of possible natural disaster.

2. To construct geodynamic model of the region of possible geological catastrophe.

3. To determine the places of highest stresses and velocities in the lithosphere of potential natural hazards.

4. Detailed analysis and monitoring of stresses and velocities in concrete places of possible earthquakes.

5. Mechanical-mathematical modeling of geological structures evolution in the regions of events in connection with deep geodynamics of the lithosphere and asthenosphere.

6. Monitoring systems construction.

7. Seismic and earthquake risk assessment, management and reduction.

8. Development and use of seismic resistant constructions.

CONFLICT OF INTEREST

The author declares no conflict of interest.

ACKNOWLEDGEMENTS

The article was prepared in response to a government assignment №122022400105-9 on the topic "Forecast, modeling and monitoring of endogenous and exogenous geological processes to reduce their negative consequences".

REFERENCES

[1] Allen CR. Active faulting in northern Turkey. California Institute of Technology, California 1969; pp. 32-34.

[2] Babeshko VA, Evdokimova OV, Babeshko OM, Evdokimov VS. On the determination of the mechanical state of tectonic faults. Geology and Geophysics of the South of Russia 2022; 12(2): 53-66.

[3] Babeshko VA, Babeshko OM, Gorshkova EM, Evdokimova OV, Zaretskaya MV, Pavlova AV, Telyatnikov IS, Fedorenko AG, Shestopalov V. L Target and interdisciplinary results of the project "Development of a complex of mathematical models for earthquake prediction with a wide range of lithospheric plates covering various types of coastal areas." In the collection: Patterns of formation and impact of marine, atmospheric hazardous phenomena and disasters on the coastal zone of the Russian Federation in the context of global climatic and industrial challenges ("Hazardous Phenomena - III"). Proceedings of the III International Scientific Conference in memory of Corresponding Member of the Russian Academy of Sciences D.G. Matishov. Rostov-on-Don, 2021; pp. 26-29.

[4] Babeshko VA, Shestopalov VL, Glazyrin EA, Sheremetiev VM. Study of seismic activity in the Greater Sochi region using satellite geodynamics methods. Science of the South of Russia 2019; 15(1): 3-11. https://doi.org/10.23885/2500-0640-2018-14-1-3-10

[5] Becker TW, Boschi L. A comparison of tomographic and geodynamic mantle models. Geochem Geophys Geosyst 2002; 3. https://doi.org/10.1029/2001GC000168

[6] Ershov AV, Nikishin AM. Recent geodynamics of the Caucasus-Arabia-East Africa region. Geotectonics 2004; 2: 55-72.

[7] Bijwaard H, Spakman W, Engdahl ER. Closing the gap between regional and global travel time tomography. J Geophys Res 1998; 103: 30055-30078. https://doi.org/10.1029/98JB02467

[8] Duman TY, *et al*. Seismotectonic database of Turkey. Bulletin of Earthquake Engineering 2018; 16(8): 3277-3316. https://doi.org/10.1007/s10518-016-9965-9

[9] Gee DG, Zeyen HJ, Eds. Europrobe 1996 - Lithosphere Dynamics: Origin and Evolution of Continents. Uppsala University 1996; p. 138.

[10] Goncharov MA, Koronovskii NV, Svalova VB, Raznitsin YuN. The contribution of mantle diapirism to the formation of newly formed basins of the Mediterranean and the Caribbean and the surrounding centrifugal-vergent folded-overlapped orogens. Geotectonics 2015; 6: 80-93.

[11] Grand SP, van der Hilst RD, Widiyantoro S. Global seismic tomography: A snapshot of convection in the Earth. GSA Today 1997; 7(4): 1-7.

[12] Güvercin SE, Karabulut H, Konca AÖ, Doğan U, Ergintav S. Active seismotectonics of the East Anatolian Fault. Geophysical Journal International 2022; 230(1): 50-69. https://doi.org/10.1093/gji/ggac045

[13] Ismail-Zadeh A, Kossobokov V. Earthquake prediction, M8 algorithm. Encyclopedia of Earth Sciences Series 2011; T. Part 5: 178-182. https://doi.org/10.1007/978-90-481-8702-7_157

[14] Khain VE, Lomize MG. Geotectonics with the basics of geodynamics. M.: KDU, 2005; p. 560.

[15] Khutorskoi MD, Antonovskaja GN, Basakina IM, Teveleva EA. Seismicity and Heat Flow in the Frame of Eastern European Platform. Volcanology and Seismology 2022; 2: 74-92. https://doi.org/10.1134/S074204632202004X

[16] Kossobokov VG, Soloviev AA. Testing earthquake prediction algorithms. Journal of the Geological Society of India 2021; T. 97. № 12: 1514-1519. https://doi.org/10.1007/s12594-021-1907-8

[17] Koulakov I, Zabelina I, Amanatashvili I, Meskhia V. Nature of orogenesis and volcanism in the Caucasus region based on results of regional tomography. Solid Earth 2012; 3: 327-337. https://doi.org/10.5194/se-3-327-2012

[18] Medved I, Koulakov I, Polat G. Crustal structure of the eastern Anatolia region (Eurkey) based on seismic tomography. Geosciences (Switzerland) 2021; T. 11. № 2: C. 1-12. https://doi.org/10.3390/geosciences11020091

[19] Medved IV, Kulakov IYu. Deep structure of the lithosphere of eastern Anatolia. In the collection: Structure of the Lithosphere and Geodynamics. Materials of the XXIX All Russian Youth Conference. Irkutsk, 2021; pp. 173-175.

[20] Milyukov VK, Mironov AP, Rogozhin EA, Steblov GM. Estimates of the speeds of modern movements of the North Caucasus from GPS observations. Geotectonics 2015; 3: 56-65. https://doi.org/10.1134/S0016852115030036

[21] Moiseenko UI, Negrov OB. Geothermal conditions of the North Caucasian seismic hazard zone. In: Geothermy of seismic and non-seismic zones. M., Science 1993; pp. 32-40.

[22] Rogozhin EA, Gorbatikov AV, Stepanova MYu, Ovsyuchenko AN, Andreeva NV, Kharazova YuV. The structure and modern geodynamics of the meganticlinorium of the Greater Caucasus in the light of new data on the deep structure. Geotectonics 2015; 2: 36-49. https://doi.org/10.1134/S0016852115020053

[23] Sharkov EV, Lebedev VA, Rodnikov AG, Chugaev AV, Sergeeva NA, Zabarinskaya LP. Features of Caucasian segment of the Alpine-Himalayan convergence zone: geological, volcanological, neotectonical, and geophysical data. In:Tectonics - Recent Advances. Editor Sharkov E. Ser. "Earth and Planetary Sciences" Rijeka, Croatia 2012; 37-50. https://doi.org/10.5772/50253

[24] Sharkov EV, Lebedev VA. Caucasian-Arabian Segment of Alpine-Himalayan Convergence: an Example of Continental Collision above Mantle Plume. Heat-Mass Transfer and Geodynamics of the Lithosphere. V. Svalova (ed.) Springer book: 89082526, 2021; pp. 381-390. https://doi.org/10.1007/978-3-030-63571-8_21

[25] Sharkov E, Svalova V. Geological-geomechanical simulation of the Late Cenozoic geodynamics in the Alpine-Mediterranean mobile belt. New Frontiers in Tectonic Research – General Problems, Sedimentary Basins and Island Arcs. INTECH, Croatia 2011; pp. 18-38. https://doi.org/10.5772/25250

[26] Sharkov EV, Svalova VB. Intracontinental seas as a result of back-arc spreading with a collision of continental plates. Reports of the USSR Academy of Sciences 1989; 308(3): 685-688.

[27] Sharkov EV, Svalova VB. On the possibility of involving the continental lithosphere in the subduction process during back-arc spreading. Izv. AN USSR, ser.geol. 1991; 12: 118-131. https://doi.org/10.1080/00206819109465745

[28] Sherman SI. Deformation waves as a trigger mechanism of seismic activity in seismic zones of the continental lithosphere. Geodynamics & Tectonophysics 2013; 4(2): 83-117. https://doi.org/10.5800/GT-2013-4-2-0093

[29] Stein RS, Barka AA, Dieterich JH. Progressive failure on the North Anatolian fault since 1939 by earthquake stress triggering. Geophysical Journal International 1997; 128(3): 594-604. https://doi.org/10.1111/j.1365-246X.1997.tb05321.x

[30] Stern RJ, Johnson P. Continental lithosphere of the Arabian Plate: A geologic, petrologic, and geophysical synthesis. Earth-Science Reviews 2010; 101: 29-67. https://doi.org/10.1016/j.earscirev.2010.01.002

[31] Svalova VB. Management of geoenvironmental risk and problems of sustainable development of mountain territories. Geology and Geophysics of the South of Russia 2022; 12(1): 129-147. https://doi.org/10.46698/VNC.2022.48.61.010

[32] Svalova V, Ed. Earthquakes - Forecast, Prognosis and Earthquake Resistant Construction. InTech, 2018. https://doi.org/10.5772/intechopen.71298

[33] Svalova V. Earthquakes: Life at Risk. In: Svalova V. (editor).Earthquakes - Forecast, Prognosis and Earthquake Resistant Construction. InTech. 2018. https://doi.org/10.5772/intechopen.71298

[34] Svalova VB. Mechanical-mathematical models of the formation and evolution of sedimentary basins. Sciences de la Terre, Ser. Inf., 1992; 31: 201-208.

[35] Svalova VB. Mechanical-mathematical simulation of geological structures evolution. Geoinformatics 1993; 4(3): 153-160. https://doi.org/10.6010/geoinformatics1990.4.3_153

[36] Svalova VB. Thermomechanical modeling of geological structures formation and evolution on the base of geological-geophysical data. Proceedings of the Third Annual Conference of the International Association for Mathematical Geology IAMG'97, Barcelona, Spain 1997; Part 2: 1049-1055.

[37] Svalova V. Mechanical-mathematical modeling for the Earth's deep and surface structures interaction. Proceedings of International Conference IAMG, Berlin 2002; p. 5.

[38] Svalova VB. Mechano-mathematical modeling of the formation and evolution of geological structures in connection with deep mantle diapirism. Monitoring. Science and Technology 2014; 3(20): 38-42.

[39] Svalova VB, Sharkov EV. Formation and evolution of back-arc basins of the Alpine and Pacific belts (comparative analysis). Pacific Geology 1991; 5: 49-63.

[40] Svalova VB, Sharkov EV. Geodynamics of the Baikal rift zone (petrological and geomechanical aspects). Geology and Geophysics 1992; 5: 21-30.

[41] Svalova VB, Zaalishvili VB, Ganapathy GP, Nikolaev AV, Melkov D. A Landslide risk in mountain areas. Geology of the South of Russia 2019; 9(2): 109-127.

[42] The Global Heat Flow Database of the International Heat Flow Commission. http://www.heatflow.und.edu/

[43] Ulomov VI, Danilova TI, Medvedeva NS, Polyakova TP, Shumilina LS. To the assessment of seismic hazard in the North Caucasus. Physics of the Earth 2007; 7: 31-45. https://doi.org/10.1134/S1069351307070051

[44] Zanemonetz (Svalova) VB, Kotelkin VD, Miasnikov VP. On the dynamics of lithospheric movements. Izvestia of the USSR Ac. Sci., Ser. Physics of the Earth 1974; 5: 43-54.

[45] Zhao D. Seismic structure and origin of hotspots and mantle plumes. Earth Planet Sci Let 2001; 192: 423-436. https://doi.org/10.1016/S0012-821X(01)00465-4

[46] Zhou H A high-resolution P wave model for the top 1200 km of the mantle. J Geophys Res 1996; 101: 27791-27810. https://doi.org/10.1029/96JB02487

[47] Zoback M. Reservoir Geomechanics. Cambridge University Press, New York 2007; p. 505. https://doi.org/10.1017/CBO9780511586477

[48] Zoback ML. First and second order patterns of tectonic stress: The World Stress Map Project. Journal of Geophysical Research 1992; 97: 11,703-11,728. https://doi.org/10.1029/92JB00132